

# Effect of thermal $^3\text{He}$ minorities on knock-on tail formation and the resulting neutron emission spectrum modification in deuterium-tritium plasmas

Matsuura, Hideaki

Department of Applied Quantum Physics and Nuclear Engineering, Kyushu University

Nakamura, M.

Department of Frontier Sciences, University of Tokyo

Mitarai, O.

Liberal Arts Education Center, Kumamoto Campus, Tokai University

Nakao, Y.

Department of Applied Quantum Physics and Nuclear Engineering, Kyushu University

<https://hdl.handle.net/2324/25465>

---

出版情報 : Plasma Physics and Controlled Fusion. 53 (3), pp.035023(1)-035023(11), 2011-02-10.  
IOP

バージョン :

権利関係 : (C) 2011 IOP Publishing Ltd



# Effect of thermal $^3\text{He}$ minorities on knock-on tail formation and the resulting neutron emission spectrum modification in deuterium-tritium plasmas

by

H. Matsuura<sup>1</sup>, M. Nakamura<sup>2</sup>, O. Mitarai<sup>3</sup> and Y. Nakao<sup>1</sup>

<sup>1</sup>Department of Applied Quantum Physics and Nuclear Engineering,  
Kyushu University, 744 Motooka, Fukuoka 819-0395, Japan

<sup>2</sup>Department of Frontier Science, the University of Tokyo,  
5-1-5 Kashiwa, Chiba 277-8561, Japan

<sup>3</sup>Liberal Arts Education Center, Kumamoto Campus, Tokai University,  
9-1-1 Toroku, Kumamoto 862-8652, Japan

e-mail: mat@nucl.kyushu-u.ac.jp

(Dated: January 7, 2011)

## Abstract

The knock-on tail formations in fuel-ion velocity distribution functions by energetic alpha-particles (by the  $\text{T(d,n)}^4\text{He}$  reaction) and protons (by the  $\text{D(d,p)}\text{T}$  and  $^3\text{He(d,p)}^4\text{He}$  reactions) are investigated by simultaneously solving the Boltzmann-Fokker-Planck (BFP) equations for deuteron, triton,  $^3\text{He}$ , alpha-particle and proton in an ITER-like deuterium-tritium (DT) plasma admixed with a small amount of  $^3\text{He}$ . As a result of the  $^3\text{He}$  inclusion, fraction of the transferred energy from energetic ions to thermal deuterons and tritons via nuclear plus interference (NI) scattering is reduced. Owing to the NI scattering of the energetic protons by fuel-ions, the latter are knocked up to higher energies. The knocking-up effect of fuel ions is enhanced with increasing  $^3\text{He}$  concentration. It is shown that if  $^3\text{He}$  with relative concentration of 4.2 %, i.e.  $n_{^3\text{He}}/n_e = 0.042$ , is included in  $T_e = 20$  keV,  $n_e = 9.5 \times 10^{19} \text{ m}^{-3}$  plasma, the magnitude of the knock-on tail in deuteron distribution function in 300 keV~3 MeV energy range is reduced by about 15 % from the value when  $^3\text{He}$  is not externally supplied. Such knock-on tail reduction also results in alternation of the non-Gaussian neutron emission spectrum with energies less than ~13 MeV and above ~15 MeV.

(PACS number: 52.55-s, 52.55-Pi, 28.52-s)

---

Prepared for submission to Plasma Physics and Controlled Fusion

## 1. Introduction

In a deuterium-tritium (DT) plasma knock-on tails are created in fuel-ion velocity distribution functions due to nuclear elastic scattering [1,2] of energetic alpha-particles. In thermonuclear plasmas, alpha-particles play an important role in attaining and sustaining the plasma, and aiming at an application to the alpha-particle diagnostics, the resulting modification of the neutron emission spectrum has been computed [3] and experimentally ascertained [4,5].

For study of burning plasmas like ITER, the evaluation of capability for confined alpha-particle diagnostics is a crucial issue. Spectroscopic measurement techniques, such as collective Thomson scattering (CTS) and neutron emission spectrum, are promising ways for the confined alpha-particle diagnostics [6,7] and the techniques will be implemented in ITER [7]. Large Doppler shifts in CTS and neutron energy spectrum are used for diagnostics of the energy distribution function of the confined alpha-particles. It is important for such spectroscopic diagnostics to discriminate between alpha-particle and other energetic particle signals. In ITER-like burning plasmas, such energetic particles are generated due to neutral beam injection (NBI) and ion cyclotron range of frequency (ICRF) heating. In ITER use of deuterium-beam energy up to 1 MeV is planned and the ICRF heating with  $^3\text{He}$  minorities has been considered to be one of the most promising plasma heating schemes [8,9]. The NBI effects on the Doppler shifts have been evaluated for CTS [10] and neutron emission spectrum [11] diagnostics, and such effects have been found to be insignificant, since the energy range of NBI is, at most, about 1 MeV. On the other hand, ICRF heating with  $^3\text{He}$  minority could be problematic for the spectroscopic alpha-particle diagnostics since  $^3\text{He}$  minority ions are accelerated up to the MeV energy range. Salewski et al [12] found that the energetic  $^3\text{He}$  minorities can contribute to the large Doppler shifts in CTS spectra and can interfere with the alpha-particle distribution measurement. Nevertheless, such a  $^3\text{He}$  effect would not spoil the spectroscopic alpha-particle diagnostics in an entire plasma region since the effect is limited within a region

originated from ICRF resonance layer on the specific magnetic flux surface [12]. In the ICRF heating schemes, the energetic  $^3\text{He}$  minorities are also contribute to the knock-on tail formation in fuel-ion distribution function. Zaitsev et al. [13] evaluated the knock-on tail formation in the deuterium distribution function due to the ICRF-heated  $^3\text{He}$  minorities in their modeling of the JET deuterium plasma experiments. Such a knock-on tail due to the heated  $^3\text{He}$  minorities could be appreciable although the knock-on tail evaluated was underestimated compared with the experimental results. Interference by the heated  $^3\text{He}$  minorities, therefore, could occur in neutron emission spectrum measurements, as well as CTS, in ITER. The contribution of  $^9\text{Be}$ -concerning reactions on CTS has also been evaluated [14]. From the viewpoint of confined alpha-particle diagnostics, clarification of how such a plasma operation (heating scheme) influences the plasma diagnostic scenarios is important and currently it becomes one of the most interesting topics.

In this paper we examine the influences of “unheated, thermal  $^3\text{He}$  minorities” on the alpha-particle diagnostic scenarios using neutron emission spectrum. It should be kept in mind that the effect of the thermal  $^3\text{He}$  minorities extends not only in the ICRF resonance layer but also in the whole burning plasma region. In DT plasmas, protons are intrinsically produced by the side, i.e. the  $\text{D(d,p)T}$ , reaction. When a small amount of  $^3\text{He}$  are admixed, e.g. for the purpose of the minority heating experiments, the protons produced by the  $^3\text{He(d,p)}^4\text{He}$  reaction also contribute to the knock-on tail formation. Owing to the  $^3\text{He}$  inclusion, fraction of the transferred power from fusion-produced alpha-particles to bulk deuterons and tritons via both nuclear plus interference (NI) and Coulomb scattering is relatively reduced, which would cause the reduction in the magnitude of the knock-on tail in fuel-ion distribution functions. A new effect considered in this paper for the first time is that the nuclear elastic scattering of the energetic protons produced by the  $\text{D(d,p)T}$  and  $^3\text{He(d,p)}^4\text{He}$  reactions would also knock up the fuel-ions (once scattered up by energetic alpha-particles) to further

high-energy range. These processes may influence the knock-on tail formation in fuel-ion distribution functions and the resulting neutron-emission-spectrum modification processes. If the energetic component of the neutron emission spectrum, i.e.  $> \sim 15$  MeV, changes its shape from the values evaluated without considering the effect of  $^3\text{He}$  inclusion, plasma diagnostics scenarios utilizing the energetic neutrons may be affected. The effect of nuclear elastic scattering in a neutral-beam-injected plasma [15-17] and the modification of alpha-particle emission spectrum have been studied [18]. The knock-on tail formation in ICRF heated plasmas by resonated energetic ions has also been examined [13]. In addition to these studies, the influences of the thermal  $^3\text{He}$  inclusion on the spectrum modification process should also be quantitatively grasped by considering the contribution of fusion-produced energetic protons in DT plasmas.

A DT plasma with a small amount of  $^3\text{He}$  admixture is considered. ICRF heating accelerates ions to high-energy range, leading to strongly anisotropic fast ion distribution functions [13]. In such a state, the spectrum of fusion-produced neutrons itself would change its shape from the one without considering such external heating processes. However, since the influences of the distortion of the fuel-ion distribution function on the shape of the energetic alpha-particle and proton slowing-down distributions would be small, the relative change in the neutron emission spectrum (caused by knock-on collision of energetic alpha-particle and proton) as a result of the thermal  $^3\text{He}$  inclusion would not be affected by the external heating processes so much. In this paper we solve the Boltzmann-Fokker-Planck (BFP) equations [16,17,19] for deuteron, triton,  $^3\text{He}$ , alpha-particle and proton without considering the resonance process with injected RF waves. The knock-on tail formations in fuel-ion distribution functions by energetic alpha-particles and protons, and resulting modification in neutron emission spectrum are evaluated. A recognizable change in the neutron emission spectrum due to thermal  $^3\text{He}$  inclusion is revealed.

## 2. Analysis model

The BFP equation for ion species  $i$  ( $i=D, T, \text{alpha-particle, proton and } ^3\text{He}$ ) is written as

$$\sum_j \left( \frac{\partial f_i}{\partial t} \right)_j^{Coulomb} + \sum_n \left( \frac{\partial f_i}{\partial t} \right)_n^{NI} + \frac{1}{v^2} \frac{\partial}{\partial v} \left( \frac{v^3 f_i}{2\tau_c^*(v)} \right) + S_i(v) - L_i(v) = 0, \quad (1)$$

where  $f_i(v)$  is the velocity distribution function of the species  $i$ . The first term in the right-hand side of Eq.(1) represents the Coulomb collision term. The summation is taken over all background species, i.e.  $j=D, T, \text{alpha-particle, proton, } ^3\text{He}$  and electron. The collision term is hence non-linear, retaining collisions between ions of the same species. The electrons are assumed to be Maxwellian with temperature  $T_e$ . The second term accounts for the nuclear elastic scattering of species  $i$  by background ion  $n$  [15,16]. We consider the nuclear elastic scattering between 1) alpha-particle and D, 2) alpha and T, 3) alpha and  $^3\text{He}$ , 4) proton and D, 5) proton and T and 6) proton and  $^3\text{He}$ , i.e.  $(i,n) = (D,\alpha), (T,\alpha), (^3\text{He},\alpha), (\alpha,D), (\alpha,T), (\alpha,^3\text{He}), (D,p), (T,p), (^3\text{He},p), (p,D), (p,T)$  and  $(p,^3\text{He})$ . The NI cross-sections are taken from the work of Perkins and Cullen [2].

The third term in the left-hand side of Eq.(1) represents the diffusion in velocity space due to thermal conduction. In this paper the unknown loss mechanism has been incorporated into the analysis by using dimensionless parameter  $\gamma$  following Bittoni's treatment [20,21], i.e.  $\tau_c^{*i}(v) = C_C^i \tau_C^i$ ,  $\tau_P^{*i}(v) = C_P^i \tau_P^i$  (when  $v < v_{th}^i$ ) and  $\tau_C^{*i}(v) = C_C^i \tau_C^i (v/v_{th}^i)^\gamma$ ,  $\tau_P^{*i}(v) = C_P^i \tau_P^i (v/v_{th}^i)^\gamma$  (when  $v \geq v_{th}^i$ ). Here  $v_{th}^i$  represents the thermal velocity of ion species  $i$ , and the coefficient  $C_C^i$  ( $C_P^i$ ) is determined so that the velocity-integrated energy (particle) loss rate becomes  $(3/2)n_i T_i / \tau_C^i$  ( $n_i / \tau_P^i$ ) for each ion species. The high exponent  $\gamma$  chosen ensures rapid increment of both energy and particle confinement times in high energy range compared with the ones in the thermal energy range. In this paper throughout the calculations  $\gamma = 4$  is assumed. As was discussed in Ref.16, as for the current study the  $\gamma$  is not an influential parameter. Considering both energy loss

mechanisms due to thermal conduction and particles transport loss from the plasma, the confinement time due to conduction loss  $\tau_C^i$  is determined for each ion species using the global energy confinement time  $\tau_E$  so that the following relation is satisfied for each species,

$$\frac{(3/2)n_i T_i}{\tau_E} = \frac{(3/2)n_i T_i}{\tau_C^i} + \int \frac{(1/2)m_i v_i^2}{\tau_P^i(v)} f_i(v_i) d\vec{v}_i . \quad (2)$$

The source ( $S_i(v)$ ) and loss ( $L_i(v)$ ) terms take different form for every ion species. For fuel deuterons, the source and loss terms can be expressed as

$$S_D(v) - \left( \frac{\partial f_D}{\partial t} \right)^R - L_D(v) = \frac{S_D}{4\pi v^2} \delta(v - v_D^{fueling}) - \sum_k \zeta_D^k(v) f_D - \frac{f_D(v)}{\tau_P^{*D}(v)} . \quad (3)$$

Here  $v_D^{fueling}$  indicates the speed of the fueled deuterium, which is much lower than the thermal speed (nearly equal to zero). The fueling rate  $S_D$  is determined so that the deuteron density is kept constant, i.e.

$$S_D = n_D / \tau_p + n_D n_T \langle \sigma v \rangle_{DT} + (1/2) n_D^2 \langle \sigma v \rangle_{DD(p)} + (1/2) n_D^2 \langle \sigma v \rangle_{DD(n)} + n_D n_{^3He} \langle \sigma v \rangle_{D^3He} . \quad (4)$$

The second term in the right-hand side of Eq.(3) represents the particle disappearance from the plasma due to fusion reactions. Here  $k$  represents a kind of reactions, i.e.  $T(d,n)^4He$ ,  $D(d,p)T$ ,  $D(d,n)^3He$  and  $^3He(d,p)^4He$ . For example, the  $\zeta_D^{DT}(v)$  ( the function for the  $T(d,n)^4He$  reaction ) can be written in the following form [19],

$$\zeta_D^{DT}(v) = \frac{2\pi}{v} \int dv_T v_T f_T(v_T) \left[ \int_{|v-v_T|}^{v+v_T} dv_r v_r^2 \sigma_{DT}(v_r) \right] . \quad (5)$$

For fuel tritons, we have to include the production term by the  $D(d,p)T$  reactions as

$$S_T(v) - \left( \frac{\partial f_T}{\partial t} \right)^R - L_T(v) = \frac{S_T}{4\pi v^2} \delta(v - v_T^{fueling}) + \frac{S_T^{DD}}{4\pi v^2} \delta(v - v_T^{DD}) - \zeta_T^k f_T - \frac{f_T(v)}{\tau_P^{*T}(v)} . \quad (6)$$

Here the  $S_T^{DD}$  represents the triton production rate by the D(d,p)T fusion reaction, i.e.

$S_T^{DD} = (1/2)n_D^2 \langle \sigma v \rangle_{DD(p)}$ , and  $v_T^{DD}$  is the triton speed corresponding to the 1.01-MeV birth energy.

The fueling rate  $S_T$  is determined so that the triton density is kept constant, i.e.

$$S_T = n_T / \tau_p + n_D n_T \langle \sigma v \rangle_{DT} - (1/2) n_D^2 \langle \sigma v \rangle_{DD(p)}. \quad (7)$$

In the same manner, for alpha-particle, proton and  $^3\text{He}$ , the source and loss terms are determined so that the fusion sources and losses due to transport and fusion reactions are balancing. It should be noted that for  $^3\text{He}$ , when we consider the external fueling to keep the  $^3\text{He}$  density at a specific value, the fueling term is included in the BFP equation and is chosen so that the total density becomes constant as was explained in Eq.(3) and (6).

By using computational iterative method, the above BFP equations for deuterons, tritons, alpha-particles, protons and  $^3\text{He}$  are simultaneously solved for given electron temperature, fuel-ion densities and global confinement times, so that global power balance and particle conservation for each ion species are satisfied. Finally we can obtain the velocity distribution functions at equilibrium state. From the obtained fuel-ion distribution functions, the neutron emission spectrum is evaluated by

$$\frac{dN_n}{dE}(E) = \iiint f_D(|\vec{v}_D|) f_T(|\vec{v}_T|) \frac{d\sigma}{d\Omega} \delta(E - E_n) |\vec{v}_D - \vec{v}_T| d\vec{v}_D d\vec{v}_T d\Omega, \quad (8)$$

where  $N_n$  represents the neutron generation rate,  $d\sigma/d\Omega$  is the differential cross section of the T(d,n) $^4\text{He}$  reaction,  $E$  represents the neutron energy in the laboratory system and  $E_n$  is its birth energy in the laboratory system according to the specific combination of  $\vec{v}_D$  and  $\vec{v}_T$ ; the expression of which has been derived [22,23] as

$$E_n = \frac{1}{2} m_n V_c^2 + \frac{m_\alpha}{m_\alpha + m_n} (Q + E_r) + V_c \cos \theta_c \sqrt{\frac{2m_\alpha m_n}{m_\alpha + m_n} (Q + E_r)}, \quad (9)$$



where  $m_{\alpha(n)}$  is the  $\alpha$ -particle (neutron) mass,  $V_c$  is the centre-of-mass velocity of the colliding fuel ions,  $\theta_c$  is the angle between the centre-of-mass velocity and the  $\alpha$ -particle (neutron) velocity in the centre-of-mass frame and  $Q$  is the reaction  $Q$ -value, i.e. 17.59 MeV. The  $E_r$  represents the relative energy of fuel ions, i.e.  $E_r = (1/2)m_D m_T / (m_D + m_T) |\vec{v}_D - \vec{v}_T|^2$ . Throughout the calculation, the cross sections for the T(d,n)<sup>4</sup>He reaction are taken from the work of Drogg [24] and Bosch [25].

### 3. Numerical results

In Fig.1 ion distribution functions for (a) deuterons, (b) tritons, (c) <sup>3</sup>He, (d) alpha-particles and (e) protons, when <sup>3</sup>He with relative concentration of 0.9, 4.2 and 7.7 %, i.e.  $n_{^3\text{He}}/n_e$  ( $n_{^3\text{He}}/n_D$ ) = 0.009 (0.02), 0.042 (0.1) and 0.077 (0.2), is included are shown together with the ones when <sup>3</sup>He is not externally supplied. In the calculation, the fuel-ion density  $n_D = n_T = 4 \times 10^{19} \text{ m}^{-3}$ , energy and particle confinement times  $\tau_E = (1/2)\tau_p = 3 \text{ sec}$  are assumed. The electrons are assumed to be Maxwellian with 20 keV temperature, and its density is evaluated as  $8.9 \sim 10.4 \times 10^{19} \text{ m}^{-3}$  depending on the <sup>3</sup>He concentrations. It is shown that the energetic non-Maxwellian component is created in alpha-particle distribution function due to its 3.52-MeV fusion source, and as a result of nuclear elastic scattering of energetic alpha-particles by bulk ions, knock-on tails are created in deuteron, triton and <sup>3</sup>He velocity distribution functions in  $\sim 500 \text{ keV} \sim 3 \text{ MeV}$  energy range. In Fig.1(e), we can also see that the energetic non-Maxwellian tail is created in proton distribution function reflecting 3.02 MeV (by the D(d,p)T reaction) and 14.7 MeV (by the <sup>3</sup>He(d,p)<sup>4</sup>He reaction) birth components. The energetic component in proton distribution function above 3 MeV energy range grows large as the <sup>3</sup>He concentration increases. Owing to the knocked-up process of bulk deuterons, tritons and <sup>3</sup>He by energetic (3~15 MeV) protons, knock-on tails are also created above  $\sim 3 \text{ MeV}$  energy range in deuteron, triton and <sup>3</sup>He velocity distribution functions. Since

the magnitude of the second knock-on tails (above  $\sim 3$  MeV energy range) in the fuel-ion distribution functions are almost proportional to the magnitude of the second tail (in 3~15 MeV energy range) in proton distribution function, we can say that the second knock-on tails (above  $\sim 3$  MeV energy range) in the fuel-ion distribution functions are mainly caused by the external  $^3\text{He}$  fueling.

As a result of the non-Maxwellian tail formations in the fuel-ion distribution functions due to nuclear elastic scattering and 0.82-MeV  $^3\text{He}$  fusion source by the  $\text{D(d,n)}^3\text{He}$  reaction, the fusion reaction rate coefficients for the  $\text{D(d,n)}^3\text{He}$ ,  $\text{D(d,p)}\text{T}$ ,  $\text{T(d,n)}^4\text{He}$  and  $^3\text{He(d,p)}^4\text{He}$  reactions are enhanced (or decreased depending on the plasma condition) from the values when Maxwellian (presented by dotted lines in Fig.1(a) ~ (e)) is assumed. In the plasma condition shown in Fig.1 ( $^3\text{He}$  concentration is 0.9~7.7 %), the degree of the enhancement in both  $\text{D(d,n)}^3\text{He}$  and  $\text{D(d,p)}\text{T}$  reaction rate coefficients from the values for Maxwellian is estimated to be about 3~6 %. The changes in the  $\text{T(d,n)}^4\text{He}$  and  $^3\text{He(d,p)}^4\text{He}$  reaction rate coefficients are roughly estimated as  $\sim 1$  % and 10~23 % respectively.

Now let's look at the fuel-ion distribution functions more precisely. The changes in the (a) deuteron, (b) triton and (c)  $^3\text{He}$  distribution functions due to  $^3\text{He}$  inclusion, i.e. the ratio of the fuel-ion distribution function when  $^3\text{He}$  is included ( $f_D^{n_{^3\text{He}}/n_e}$ ,  $f_T^{n_{^3\text{He}}/n_e}$ ,  $f_{^3\text{He}}^{n_{^3\text{He}}/n_e}$ ) to the one when no external  $^3\text{He}$  fueling is made ( $f_D^0$ ,  $f_T^0$ ,  $f_{^3\text{He}}^0$ ), are shown in Fig.2 as a function of deuteron, triton and  $^3\text{He}$  energies respectively for  $n_{^3\text{He}}/n_e$  ( $n_{^3\text{He}}/n_D$ ) = 0.009 (0.02), 0.042 (0.1) and 0.077 (0.2). The calculation condition is the same as the one in Fig.1. It should be noted that in the calculation without external  $^3\text{He}$  fuelling, a small fraction of  $^3\text{He}$  (less than 0.1 % of electron density) is still exist in the plasma as a result of production by the  $\text{D(d,n)}^3\text{He}$  fusion reaction. We can first see that the ratios rapidly increase in the energy range above  $\sim 3$  MeV in all fuel-ion distribution functions. This is due to the creation of the second knock-on tail in both deuteron and triton distribution functions in the energy

range above  $\sim 3$  MeV by protons produced by  $^3\text{He}(d,p)^4\text{He}$  reaction (see Fig.1 (a), (b) and (c)). Secondly we notice that the magnitudes of both of the deuteron and triton distribution functions decrease in the energy range between  $\sim 200$  keV and  $\sim 3$  MeV. As a result of the external  $^3\text{He}$  supplement, the  $^3\text{He}$  concentration increases; we can see the increment of bulk (plus energetic knock-on tail) component of  $^3\text{He}$  distribution function in Fig.2(c). Since the intensity of the  $^3\text{He}$  source by  $D(d,n)^3\text{He}$  reaction is not influenced by the external  $^3\text{He}$  supplement, the degree of the change in the  $^3\text{He}$  distribution function in the energy range between  $\sim 200$  keV and  $\sim 1$  MeV is relatively small. The transferred power from energetic alpha-particles to bulk fuel-ions for several  $^3\text{He}$  concentrations are indicated in Table 1. As the  $^3\text{He}$  concentration increases, the transferred power from alpha-particles to  $^3\text{He}$  is enhanced, which causes relative decrement in transferred power from alpha-particles to deuterons and tritons (knocking up rate of bulk deuterons and tritons by energetic alpha-particles via NI scattering). On the contrary, since proton density increases due to the  $^3\text{He}$  inclusion (see Fig.1(e)), the knocking up rate of bulk deuterons and tritons by energetic protons via NI scattering is enhanced as the  $^3\text{He}$  concentration increases (see Fig.1(a) and (b)).

The neutron emission spectrum is shown in Fig.3 (a) in the case without  $^3\text{He}$  fueling. The calculation condition is the same as the one in Fig.1 and 2. In Fig.3, the dotted line denotes Gaussian distribution of 20 keV temperature. The bold line shows the neutron emission spectrum produced by non-Maxwellian components in deuteron and triton distribution functions (which is obtained by subtracting the Gaussian component from the total, i.e. Gaussian plus non-Gaussian, calculated spectrum). Since both of the total and Gaussian spectrums have the same production rate, the bold line has negative value around peak, i.e.  $\sim 14$  MeV, energy range. As was already predicted in Ref.3 the non-Gaussian component is well created in the emission spectrum. In Fig.3 (b) the spectra for several  $^3\text{He}$  concentrations are shown in a different neutron energy scale. It is found that the spectrum above

~15.5 MeV energy range decreases with increasing  $^3\text{He}$  concentration. We show the relative change in the emission spectrum due to  $^3\text{He}$  inclusion from the values without  $^3\text{He}$  fueling in Fig.4 for several  $^3\text{He}$  concentrations. Here  $(dN_n/dE)_{normalized}^0$  represents the neutron emission spectrum normalized by the neutron emission rate  $N_n$  when  $^3\text{He}$  is not fueled externally. It is shown that the emission rate of neutron with birth energy less than ~12.5 MeV and more than 15.5 MeV is decreased by about 18 (30) % for 4.2 (7.7) % of  $^3\text{He}$  concentration. The non-Gaussian component in the emission spectrum corresponds to the neutrons produced by non-thermal deuterons (tritons). Owing to the reduction in the non-thermal component in deuteron and triton distribution functions between ~200 keV and ~3 MeV energy range (as was shown in Fig.1 and Fig.2), the neutron spectrum changes its shape by several dozen percents.

#### 4. Discussion and concluding remarks

The influences of  $^3\text{He}$  minority on the knock-on tail formation in the fuel-ion distribution functions and the resulting modification of the neutron emission spectrum have been investigated by simultaneously solving the Boltzmann-Fokker-Planck (BFP) equations for deuterons, tritons,  $^3\text{He}$ , alpha-particles and protons in DT plasma with  $^3\text{He}$  minorities. It is shown that when  $^3\text{He}$  with relative concentration of 4.2 %, i.e.  $n_{^3\text{He}}/n_e=0.042$ , is included in  $T_e=20$  keV,  $n_e=9.5\times10^{19}$  m $^{-3}$  plasma, the magnitude of the knock-on tail in the deuteron distribution function in 500 keV~3 MeV energy range is reduced by about 15 % and as the result the emission rate of neutron with birth energy less than ~12.5 MeV and more than ~15.5 MeV is decreased by about 18 % from the values without  $^3\text{He}$  fueling.

As discussed in Section 1, the heated  $^3\text{He}$  effect on the confined alpha-particle diagnostics based on spectroscopic techniques is limited in a particular region originated from ICRF heating layer on the specific magnetic flux surface. The important finding here is that unheated, thermal  $^3\text{He}$

minorities essentially not localized in such a particular region, but can extend to the entire core plasma region. The thermal  $^3\text{He}$  minority effect on the neutron emission spectrum, particularly in the energy range of more than 15 MeV, found in our analysis could be crucial for the confined alpha-particle diagnostics using the neutron emission spectrum. In ITER special attention should be paid to (i) accurate measurements and/or modeling of  $^3\text{He}$  concentration to analyze experimental data of the non-Gaussian neutron emission spectrum and (ii) a trade-off of  $^3\text{He}$  concentration for alpha-diagnostic and ICRF heating purposes.

In this paper we have considered the knock-on tail formation processes by the energetic alpha-particles and protons, and in the analysis distortions of fuel-ion distribution functions due to the ICRF heating have not been included. As a result of energetic tail formations due to ICRF resonance processes, the neutron emission spectrum may change its shape from the one shown in the present paper. If a large tail appears in the vertical direction relative to the magnetic field direction in the  $^3\text{He}$  distribution function, the  $^3\text{He}$  energetic tail may also contribute to the knock-on tail formation in the fuel-ion distribution functions especially in the vertical direction [13]. Since the reduction in the neutron emission spectrum in the energy range less than  $\sim 12.5$  MeV and more than  $\sim 15.5$  MeV (as presented in Fig.4) is caused mainly by the reduced alpha knock-on (and enhanced proton knock-on) process due to the inclusion of thermal  $^3\text{He}$  minorities, the relative change in the spectrum would not be affected by the non-Maxwellian component in the  $^3\text{He}$  distribution function itself created by the ion cyclotron resonance so much, as far as we look at the effect in all over the burning plasma. For the same reason, if non-Maxwellian energetic component appears in deuteron and/or triton distribution functions by ICRF heating, the effect on the relative change in the spectrum modification would be small.

Experimental confirmation of presence of proton-knock-on deuterium and tritium ions is important. In modeling of the experimental result in JET, Zaitsev et al. [13] found out the suprathermal tail exceeded by nearly an order of magnitude that expected due to NI scattering of ICRF-heated  $^3\text{He}$  projectile ions on bulk deuterium target ions. They *qualitatively* suggested the correlation with energetic protons produced by  $^3\text{He}(\text{d},\text{p})^4\text{He}$  reaction as the most plausible candidate to increase the amount of suprathermal fuel ions. The "beam-thermal"  $^3\text{He}(\text{d},\text{p})^4\text{He}$  reaction induced by the ICRF-heated  $^3\text{He}$  ions may increase the amount of energetic protons. The further energetic protons with birth energy above 15MeV may be produced via the same process as energetic ( $>3.5\text{MeV}$ ) alpha-particle productions analyzed in Ref.[18]. Simultaneous analysis of NI scattering of the ICRF-heated  $^3\text{He}$  ions and reaction-produced protons could model the experimental result in JET successfully. A further detailed analysis would be required about this point.

If the bulk temperature increases, the half-width of the Gaussian distribution is extended (the degree of the change in the half-width for 10~30keV temperature is  $\sim 400\text{keV}$ ). The influence of the temperature on the modification of the neutron emission spectrum due to  $^3\text{He}$  inclusion would not be so significant. If the production rates of energetic alpha-particles and protons are changed by the increased or decreased fuel-ion densities (and/or temperatures), the magnitude of the knock-on tail would also be influenced. However relative change in the neutron emission spectrum due to external  $^3\text{He}$  inclusion would not be affected so much, since the magnitude of the knock-on tail is changed due to increased or decreased fuel-ion densities (and/or temperatures) regardless of the existence of the external  $^3\text{He}$  supplies. Namely the relative change in the neutron emission spectrum would not be affected significantly for plasma temperature and density in usual operations.

## References

- [1] Devany J J, Stein M L 1971 *Nucl. Sci. Eng.* **46** 323-333.
- [2] Perkins S T, Cullen D E 1981 *Nucl. Sci. Eng.* **77** 20-39.
- [3] Ballabio L, Gorini G, Källne J 1997 *Phys. Rev. E* **55** 3358-3368.
- [4] Källne J, Ballabio L, Frenje J, et al. 2000 *Phys. Rev. Lett.* **85** 1246-1249.
- [5] Korotkov A A, Gondhalekar A, Akers R J 2000 *Phys. Plasmas* **7** 957-962.
- [6] Fisher R K 2004 *Rev. Sci. Inst.* **10** 3556-3558.
- [7] Donné A J H et al. 2007 *Nucl. Fusion* **47** S337-S384.
- [8] Bergeaud V, Eriksson L G, Start D F H 2000 *Nucl. Fusion* **40** 35-51.
- [9] Eester D V, Louche L, Koch R 2002 *Nucl. Fusion* **42** 310-328.
- [10] Egedal J et al. 2005 *Nucl. Fusion* **45** 191-200.
- [11] Gorini G et al. 2006 *33rd EPS Conference on Plasma Phys. Rome, June 2006 ECA Vol.30I*, P-1.109.
- [12] Salewski M, et al. 2009 *Nucl. Fusion* **49** 025006 1-8.
- [13] F.S.Zaitsev, et al. 2007 *Plasma Phys. Control. Fusion* **49** 1747-1766.
- [14] Johnson M G, et al. 2010 *Nucl. Fusion* **50** 045005 1-14.
- [15] Matsuura H, Nakao Y, Kudo K 1999 *Nucl. Fusion* **39** 145-149.
- [16] Matsuura H, Nakao Y 2006 *Phys. Plasmas* **13** 062507 1-7.
- [17] Matsuura H, Nakao Y 2007 *Phys. Plasmas* **14** 054504 1-4.
- [18] Matsuura H, Nakao Y 2009 *Phys. Plasmas* **16** 042507 1-6
- [19] Nakaumra M, et al. 2006 *J. Phys. Soc. Jpn.* **75** 024801 1-8.
- [20] Bittoni E, Cordey J G, Cox M 1980 *Nucl. Fusion* **29** 931-938.
- [21] Mirin A A, Tomaschke G P 1982 *Nucl. Fusion* **22** 1380-1382.
- [22] Lehner G, Pohl F 1967 *Z.Phys.* **207** 83-104.
- [23] Brysk H 1973 *Plasma Phys.* **15** 611-617.

- [24] Drosch M, Schwerer O, 1987 “1-3. Production of monoenergetic neutrons between 0.1 and 23 MeV: Neutron energies and cross-sections” *Handbook of Nuclear Activation Data IAEA Vienna* **83** STI/DOC/10/273, ISBN 92-0-135087-2.
- [25] Bosch H S, Hale G 1992 *Nucl. Fusion* **32** 611-631.



## Figure Captions

**Fig.1** (color online)

Distribution functions of (a) deuterons, (b) tritons, (c)  $^3\text{He}$ , (d) alpha-particles and (e) protons in a typical DT plasma with a small amount of  $^3\text{He}$ , i.e.  $n_{^3\text{He}}/n_e$  ( $n_{^3\text{He}}/n_D$ ) = 0.009 (0.02), 0.042 (0.1) and 0.077 (0.2). The electron temperature is 20keV, fuel-ion density  $n_D = n_T = 4 \times 10^{19} \text{ m}^{-3}$ , energy and particle confinement times  $\tau_E = (1/2)\tau_p = 3 \text{ sec}$  are assumed.

**Fig.2** (color online)

Relative comparison of (a) deuteron, (b) triton and (c)  $^3\text{He}$  distribution functions when  $^3\text{He}$  with relative concentration of 0.9, 4.2 and 7.7 % is included, i.e.  $n_{^3\text{He}}/n_D = 0.02, 0.1$  and  $0.2$ , from the values without  $^3\text{He}$  fueling. The electron temperature is 20keV, fuel-ion density  $n_D = n_T = 4 \times 10^{19} \text{ m}^{-3}$ , energy and particle confinement times  $\tau_E = (1/2)\tau_p = 3 \text{ sec}$  are assumed.

**Fig.3** (color online)

Neutron emission spectra as a function of neutron energy in the laboratory system, (a) when no external  $^3\text{He}$  fueling is made and (b) for several  $^3\text{He}$  concentrations. The dotted line denotes the Gaussian distribution for 20keV temperature. The bold line in Fig.3 (a) is obtained by subtracting Gaussian component from the calculated total spectrum. The electron temperature is 20keV, fuel-ion density  $n_D = n_T = 4 \times 10^{19} \text{ m}^{-3}$ , energy and particle confinement times  $\tau_E = (1/2)\tau_p = 3 \text{ sec}$  are assumed.

**Fig.4** (color online)

Relative comparison of neutron emission spectrum when  $^3\text{He}$  with relative concentration of 0.9, 4.2 and 7.7 % is included, i.e.  $n_{^3\text{He}}/n_D = 0.02, 0.1$  and  $0.2$ , from the values when  $^3\text{He}$  is not externally supplied. The electron temperature is 20keV, fuel-ion density  $n_D = n_T = 4 \times 10^{19} \text{ m}^{-3}$ , energy and particle confinement times  $\tau_E = (1/2)\tau_p = 3 \text{ sec}$  are assumed.

**Table 1.** Transferred power from alpha-particles to fuel ions  
via nuclear elastic scattering

${}^3\text{He}/n_e ({}^3\text{He}/n_D)$	$\alpha \rightarrow D$ [kW/m <sup>3</sup> ]	$\alpha \rightarrow T$ [kW/m <sup>3</sup> ]	$\alpha \rightarrow {}^3\text{He}$ [kW/m <sup>3</sup> ]
w/o ${}^3\text{He}$ fueling	2.96	1.99	$3.73 \times 10^{-4}$
0.009 (0.02)	2.92	1.96	$2.75 \times 10^{-2}$
0.042 (0.1)	2.74	1.84	$1.29 \times 10^{-1}$
0.077 (0.2)	2.53	1.70	$2.39 \times 10^{-1}$

Figure 1 H.Matsuura, et al.

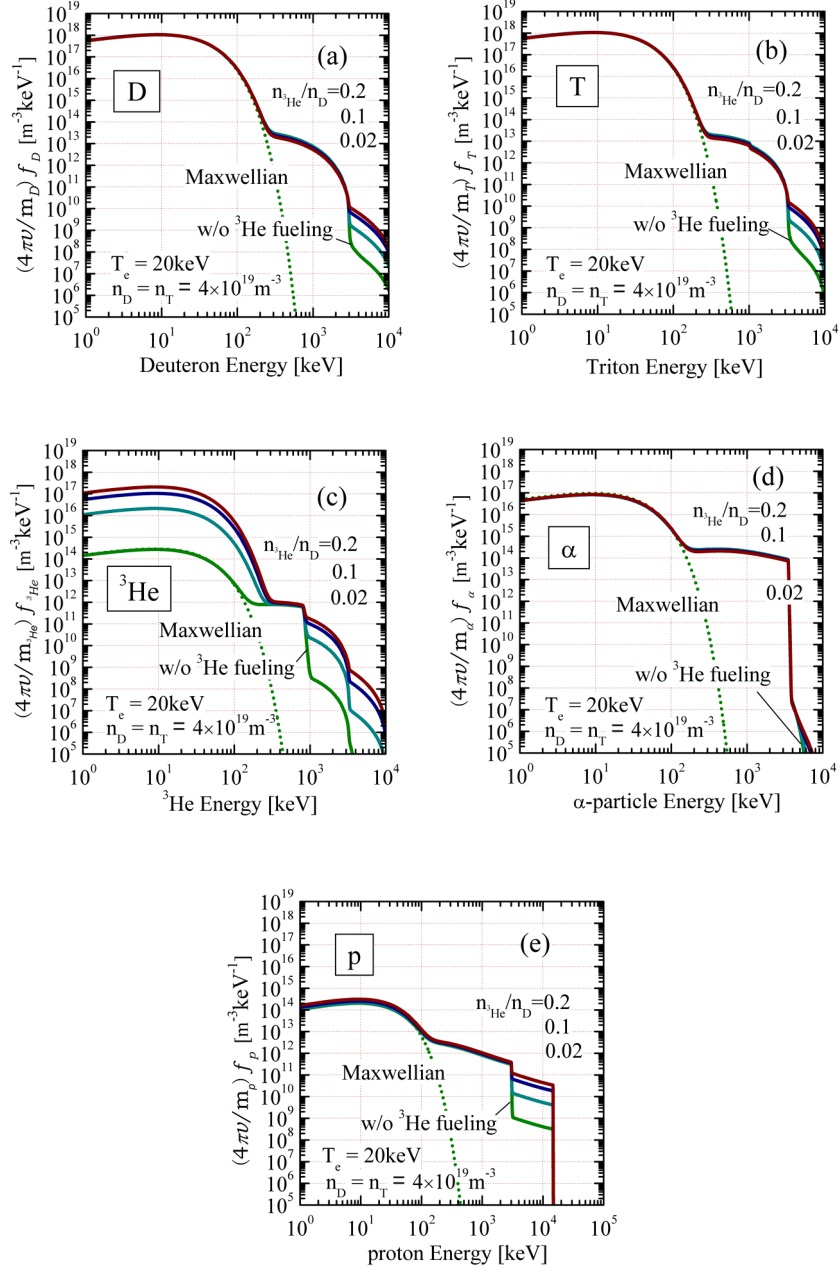


Figure 2 H.Matsuura, et al.

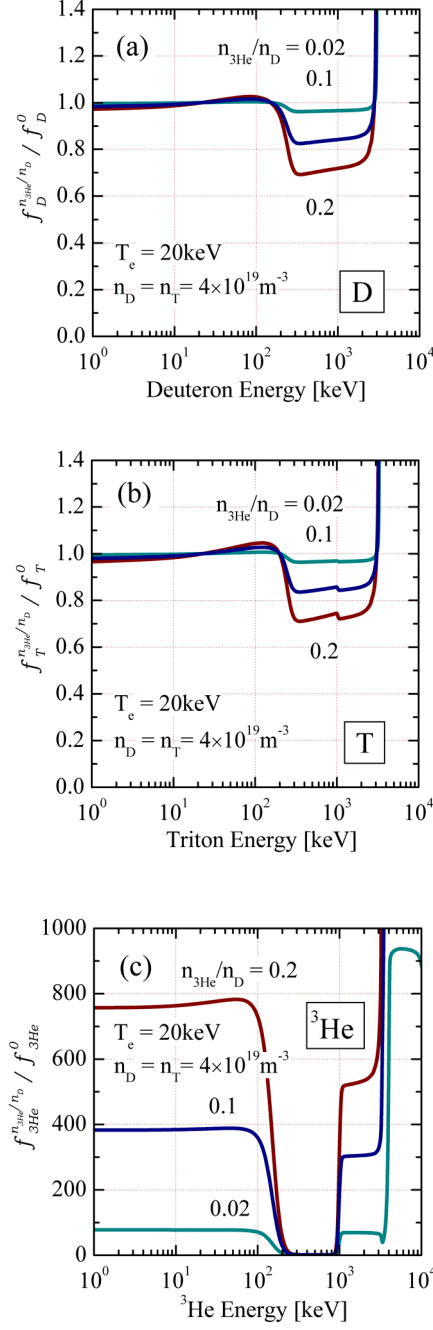


Figure 3 H.Matsuura, et al.

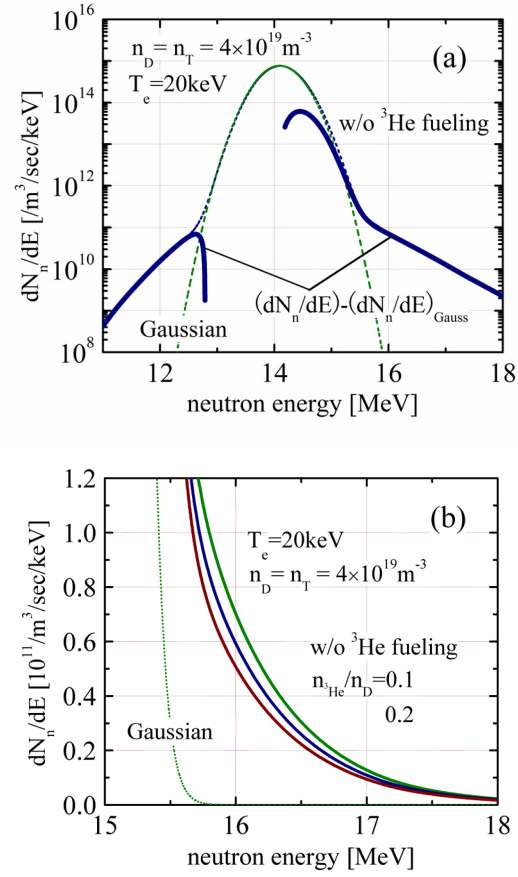


Figure 4 H.Matsuura, et al.

